



# Improvement to the Analytical Method for Dam Breach Flood Evaluation

Zuyu Chen<sup>1</sup>(✉), Lin Wang<sup>2</sup>, Xingbo Zhou<sup>3</sup>, and Shujing Chen<sup>4</sup>

<sup>1</sup> Department of Geotechnical Engineering, China Institute of Water Resources and Hydropower Research, Beijing 100048, China  
chenzuyu@cashq.ac.cn

<sup>2</sup> College of Water Resources and Hydropower Engineering, Xi'an University of Technology, Xi'an 710048, China  
ruoshuiya@163.com

<sup>3</sup> China Renewable Energy Engineering Institute, Beijing 100120, China  
zhou\_xingbo@126.com

<sup>4</sup> National Academy for Mayors of China, Beijing 100029, China  
chenshujing1991@163.com

**Abstract.** This paper describes the improvements to the existing dam breach analysis methods based on back analyses of several giant barrier lake breaches. The main improvements include a hyperbolic soil erosion model, an empirical approach to lateral enlargement modeling, and a numerical algorithm that adopts velocity increment to allow straight forward calculation for the breach flood hydrograph. It has been shown that the calculated peak flow using this improved method is less sensitive to the input parameters. The new method has been incorporated into an Excel spreadsheet DB-IWHR which is transparent, open-source, self-explanatory and downloadable on the web.

**Keywords:** Dam breach · Flood evaluation · Soil erosion

## 1 Introduction

Evaluation of the breach flood of earthen dams and levees due to overtopping is a subject of common concern that attracted a large volume of research works [1–6]. However, their physical models and numerical approaches are still unmaturing to-date. Chen et al. [7] discussed the difficulties involved in establishing the physical model that couples the disciplines of soil erosion in hydraulics and slope stability in soil mechanics. Further, shortage of field monitoring hydrographs of dam breaches makes it difficult to validate the analytical approaches developed by various researchers.

China has recently experienced a large number of barrier lake break cases with several well-documented field measured breach hydrographs [8–11]. This has allowed an in-depth study and improvements to the existing dam breach analytical methods. The research outcomes were incorporated into an Excel/VBA spreadsheet that provides an easy and quick access for practicing engineers to work during an impending dam failure emergency. A comprehensive review of this work has been presented in a latest paper [7]. This paper summarizes the key novel technical approaches in its work.

## 2 Soil Erosion Models

### 2.1 Relationship Between the Erosion Rate and Shear Stress

The relationship between the rate of soil erosion and the shear stress is a fundamental problem that has great impact on the dam breach analytical results. The relevant studies include the effort in developing better soil erosion models and apparatuses for performing the erosion tests [12].

The decrease in the channel bed elevation due to erosion per unit time,  $\dot{z}$ , can be related to the shear stress  $\tau$  on the eroded bed surface, as follows:

$$\dot{z} = \frac{\Delta z}{\Delta t} = \Phi(\tau) \quad (1)$$

where  $z$  is the channel bed elevation and  $t$  is time. The function  $\Phi(\tau)$  proposed by researchers can be divided into the following categories.

**Linear Relationship.** This model is expressed as

$$\dot{z} = \frac{\Delta z}{\Delta t} = a_L(\tau - \tau_c) \quad (2)$$

where  $\tau_c$  is the shear stress associated with the incipient velocity  $V_c$ , and  $a_L$  is the detachment rate coefficient [6, 13–15].

**Power Law Relationship.** There are a number of computer programs using the relationships based on the sedimentation dynamics, such as BREACH [5], BEED [16], and MIKE11 [17]. In general, the power relationship is [18]

$$\dot{z} = \frac{\Delta z}{\Delta t} = \Phi(\tau) = a_1(\tau - \tau_c)^{b_1} \quad (3)$$

where  $\dot{z}$  is the erosion rate in  $10^{-3}$  mm/s,  $\tau$  is in Pa,  $t$  is in second, and  $a_1$  and  $b_1$  are coefficients either regressed from the test results or based on experience. Zhou et al. [19] compares the predicted soil erosion rates from 16 models with the measured rates in Tangjiashan Barrier Lake, as shown in Fig. 1.

**Hyperbolic Relationship.** The preceding mentioned linear and power models have been developed via extensive testing works based on the theory of sedimentation dynamics and validated mostly in laboratory at low flow velocity for fine materials. It is difficult to verify these models in a real dam breach, in which the flow velocity can reach 5 m/s or more and the eroded soils contain large rock fragments. As shown in Fig. 1, it can be seen that at low shear stress, the predictions from these models more or less agree with the measured data. However, for the maximum flow velocity when the corresponding shear stress is near the peak, the power law relationship continues to predict high erosion rate. Further, the soil erosion rate is very sensitive to even a small change in the exponent  $b_1$  in Eq. (3).

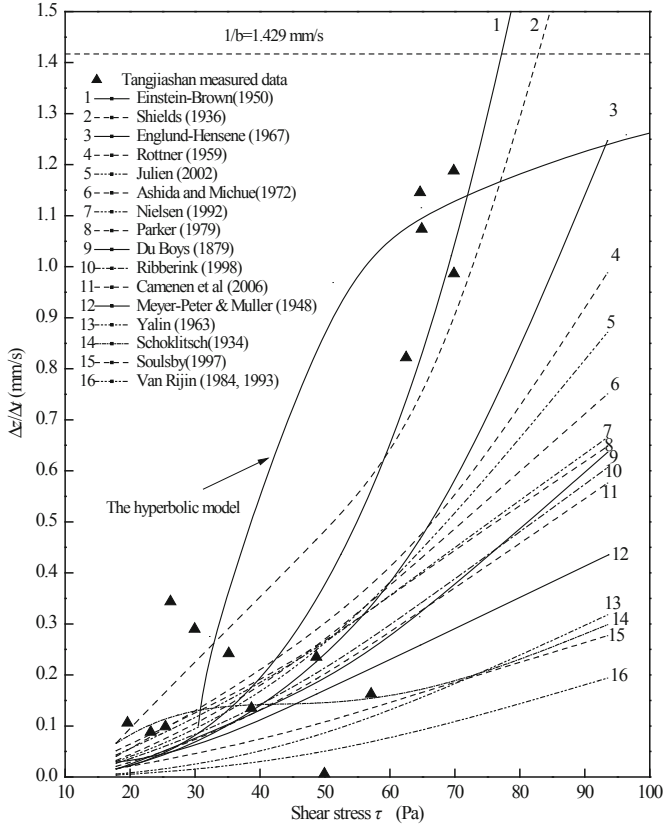


**Fig. 1.** Comparison of measured soil erosion rates with predicted rates by 16 models in Tangjiashan Barrier Lake. NOTE: According to the data of Tangjiashan barrier lake, the input parameters of this Figure are: water density,  $\rho = 1000 \text{ kg/m}^3$ ;  $\rho_s = 2650 \text{ kg/m}^3$ ; the medium size,  $d_{50} = 5 \text{ mm}$ ; roughness coefficient,  $n = 0.025$ ; void ratio,  $e = 0.36$ ; flow velocity,  $V = (2.36, 2.50, 3.99, 4.61, 5.90) \text{ m/s}$  and the corresponding the depth of water in channel,  $h = (6.94, 7.49, 8.06, 8.19, 11.86) \text{ m}$ .

In performing the back analysis for the Tangjiashan Barrier Lake, the authors proposed a hyperbolic relationship (Fig. 2) that takes the following form [1]:

$$\dot{z} = \Phi(\tau) = \frac{v}{a + bv} \quad (4)$$

where  $v$  is the shear stress with reference to its critical component  $\tau_c$

$$v = k(\tau - \tau_c) \quad (5)$$

with a unit of Pa for  $\tau$  and  $10^{-3} \text{ mm/s}$  for  $\dot{z}$ .  $k$  is a unit conversion factor, normally takes a value of 100. The hyperbolic curve has an asymptote represented by  $1/b$  as  $v$  approaches infinity, and  $1/a$  represents the tangent of this curve at  $v = 0$ .

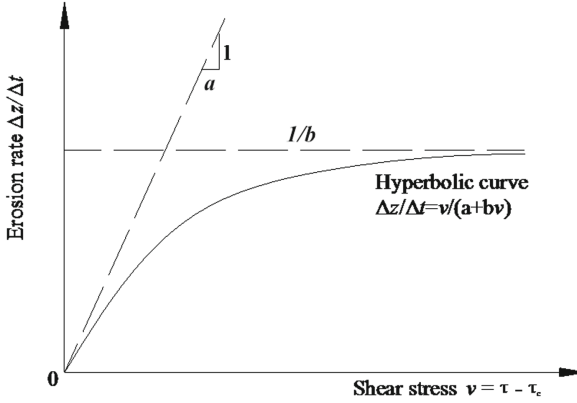


**Fig. 2.** Relationship between soil erosion rate and shear stress in the hyperbolic model.

The proposed model can be interpreted as a combination of the linear relationship with a ‘truncation’ at a certain high flow velocity. Approximately,  $1/a$  equals  $a_L$  in Eq. (2). The asymptote  $1/b$  represents the ‘strength’, which has been referred to as the ‘maximum possible erosion rate’ in this study. This is based on the understanding that for most structural materials, when the shear strength is sufficiently large, the erosion rate ‘yields’. Use of this model can prevent the calculated erosion rate becoming too large at high flow velocity. Hence, the computation results are less sensitive to the input parameters in the model. Further, since both  $1/a$  and  $1/b$  have sound physical meanings, use of these parameters can be based on common sense, which can be improved with increased knowledge. The authors collected some laboratory testing results to support this model [20].

## 2.2 Soil Erodibility Test

A variety of testing facilities have been developed as reported by Foster et al. [21], Temple [22], Shaikh et al. [23], Hanson and Simon [24], Wan and Fell [25], Zhu et al. [26], Chang and Zhang [27], and Wu [6] conducted field jet index tests to measure the erodibility of broadly graded landslide deposits and found the soil erosion resistance coefficient of Tangjiashan materials is in a range between  $0.2 \times 10^{-3}$  and  $1.2 \times 10^{-3}$  mm/s/Pa.

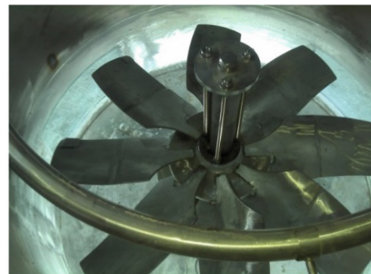
A new apparatus, called Cylindrical Erosion Test Apparatus (CETA) has been developed by the authors’ research group, as shown in Fig. 3 (Refer to Ma [28]). It includes a cylindrical, stainless steel container with an internal diameter of 1,040 mm. There are three glass windows to allow for visual inspection during the test. The propeller is driven by a speed adjustable motor with a maximum rotating speed of 1400 r/min. Similar to EFA, the soils under test is contained in a 160 mm long, 80 mm wide box, which can be lifted up to 150 mm manually as the erosion proceeds. Using a pitot tube and the FP111 direct-reading velocity meter, the reel rotating rate has been calibrated to relate to the flow velocity on the soil/water surface (refer to Fig. 4). Figure 5 shows the test results of a medium size sand with  $d_{50} = 8$  mm. The dry density is  $1.8 \text{ g/cm}^3$ .



**Fig. 3.** The Cylindrical Erosion Test Apparatus (CETA).



(a)



(b)



(c)



(d)

**Fig. 4.** Parts of CETA: (a) Speed adjustable motor (b) propeller (c) manually operated slot (d) box containing soils fixed in the slot.

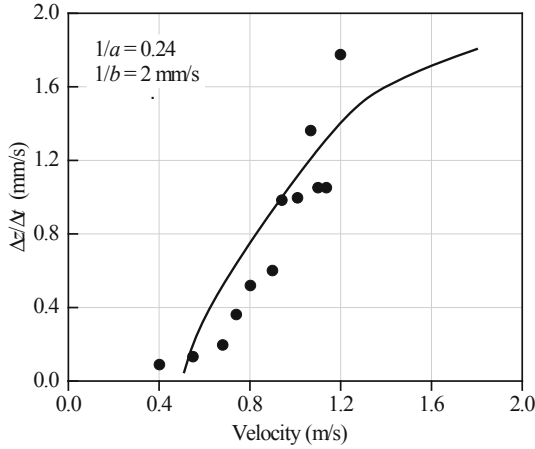


**Fig. 5.** Erodibility test results of sandy soil. NOTE: The solid line represents a regression curve based on the hyperbolic model. The asymptote  $1/b$  was postulated due to the limitation of insufficiently large flow velocity.

### 3 Modeling Lateral Enlargement

#### 3.1 Slope Stability of the Channel Banks

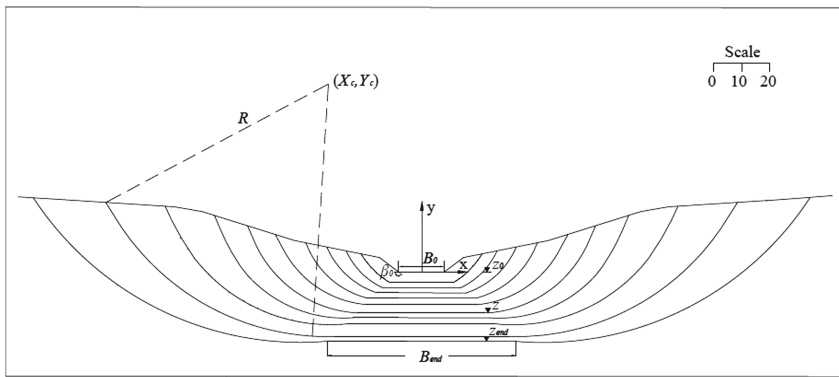
During the breach, the banks of the discharge channel collapse due to soil erosion that cut the toes. The wedge slide method has been commonly used in various dam breach models to model the processes in destabilizing the bank and widening the discharge channel (Singh and Scarlatos [29]). From the geotechnical point of view, the straight-line slip surface employed in this method is not representative of the actual failures observed in the field. It is better to replace the straight lines with a more generalized shape, such as a circular arc. Apart from this limitation, Wang et al. [30] also discussed the other drawbacks in the existing dam breach models, such as:

- (1) A majority of the existing models fails to consider the existence of a vertical cut at the slope toe which is the key factor that destabilizes the bank.
- (2) The method of determining the critical slip surface has not been clearly formulated. Wang et al. [30] discussed the proposed method by Osman and Thorne [31] who did consider the locations of the toe cut and the critical slip surface. However, they tried to find the critical toe-cutting depth by the derivatives with respect to the cohesion value of the material, which is physically unacceptable from geotechnical point of view. It is necessary to adopt the well accepted knowledge in soil mechanics that the critical slip surface is obtained by finding the minimum factor of safety associated with the geometrical coordinates that define the shape and location of the failure surface [32, 33].
- (3) The pore water pressure has been invariably ignored in the analysis. The dam body prior to a breaching failure is normally saturated if the material is impervious, such as the earth core or tailings. Hence, in the analysis, the pore pressure development that causes sudden changes in the stress field need proper treatment, both in effective stress and in total stress [34–36].

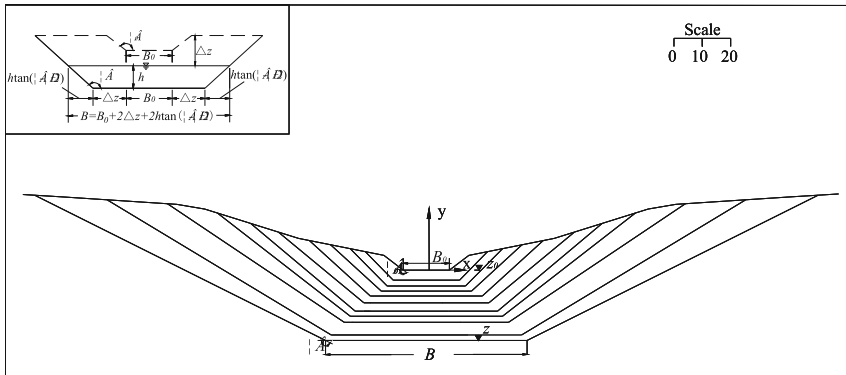
### 3.2 Improved Approaches

In view of the drawbacks, Wang et al. [30] have made the effort to improve the model based on modern geotechnical expertise which includes: (1) stability analysis with circular slip surfaces using Bishop's simplified method, (2) assignment of a vertical cut at the toe, (3) a search technique to find the minimum factor of safety and the critical depth of toe cutting, and (4) an option for determining total stress and effective stress. Figure 6(a) shows an example that is circular slip surface of modeling lateral enlargement.

Although the lateral enlargement simulation offers better geotechnical background (Fig. 6(a)), the details of the 10 steps of circular arcs as input to a computer program are too tedious for a dam breach analysis. Wang et al. [30] found that without too much loss in accuracy, the circular arc can be simplified as a straight line as shown in Fig. 6(b).



(a)



(b)

**Fig. 6.** Modeling lateral enlargement: (a) circular slip surfaces (b) straight line simplifications.

Based on an extensive regression work, Chen et al. [37] suggested an empirical hyperbolic relationship to determine the channel width associated with the channel bed elevation  $z$ , refer to Fig. 6(b).

$$B = B_0 + 2\Delta z + 2h \tan\left(\beta - \frac{\pi}{2}\right) \quad (6)$$

where

$$\Delta z = z - z_0 \quad (7)$$

and

$$\beta = \beta_0 + \Delta\beta = \beta_0 + \frac{\Delta z}{m_1 \Delta z + m_2} \quad (8)$$

$\beta$  is the slope of the channel bed,  $z_0$  and  $\beta_0$  are initial values of bed elevation and bank inclination respectively.  $m_1$  and  $m_2$  are parameters of the hyperbolic relationship which are functions of cohesion  $c$ , coefficient of friction  $\tan\phi$  and the soil bulk density  $\gamma$ . Empirical charts for determining  $m_1$  and  $m_2$  have been provided by the authors.

## 4 Numerical Modeling of Sam Breach Flood

### 4.1 Governing Equations

The numerical model considers the balance of water quantity, the continuous vertical toe cutting and lateral enlargement, which can be formulated as follows.

**Conservation of Energy and Mass.** This condition necessitates the balance between the volumes of inflow through the breach, which is normally calculated by the broad-crested weir flow equation, and the reduction of the reservoir storage per unit time, as follows:

$$Q = CB(H - z)^{3/2} = \frac{\Delta W}{\Delta H} \frac{\Delta H}{\Delta t} + q \quad (9)$$

where  $C$  is the discharge coefficient whose theoretical value is  $1.7 \text{ m}^{1/2}/\text{s}$  [29]. Earlier studies have used values of  $C$  ranging from 1.3 to 1.7 [38].  $H$  is the reservoir water elevation (Fig. 7, Chen et al. [1]), and  $q$  is the natural inflow into the reservoir.

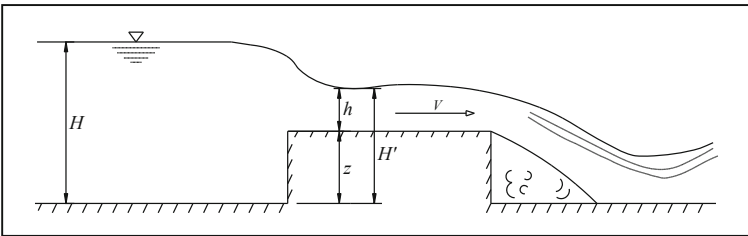


Fig. 7. Flow over a broad-crested weir.



**Constitutive Model of Soil Erodibility.** The formula describing the rate of channel bed erosion has been given in Eq. (4) in which the shear stress can be calculated using Manning equation, as follows:

$$\tau = \gamma R' J = \frac{\gamma n^2 V^2}{R'^{\frac{1}{3}}} \approx \frac{\gamma n^2 V^2}{h^{\frac{1}{3}}} \quad (10)$$

where  $\gamma$  is the density of water,  $n$  is the roughness coefficient ( $= 0.025 \text{ m}^{-1/3} \cdot \text{s}$  in this study),  $J$  is the slope of the channel, and  $R'$  is the hydraulic radius that can be approximated by  $h$  if the channel width  $B$  is sufficiently larger than the average flow depth  $h$ .

**Determination of Water Depth Behind the Weir.** The water level normally drops at the entrance of the weir if the flow is not submerged by the tailwater. Therefore, it is necessary to determine the flow depth  $h$  as shown in Fig. 7. Assuming the steady, uniform flow through the discharge channel, using Manning equation, Singh and Scarlatos [29] developed the following formula to determine  $h$ :

$$h = \left( \frac{nQ}{BJ^{0.5}} \right)^{0.6} \quad (11)$$

Use of this equation requires an input of  $J$  which is difficult to be properly defined in a dam breach problem. Experience has shown that this parameter is very sensitive to the calculated peak flow. Chen et al. [1] found that Eq. (11) can be further elaborated as

$$h = \left( \frac{nQ}{BJ^{0.5}} \right)^{0.6} = \left( \frac{nC(H-z)^{1.5}}{J^{0.5}} \right)^{0.6} = \frac{n^{0.6} C^{0.6} (H-z)^{0.9}}{J^{0.3}} \quad (12)$$

The exponent of  $(H-z)$  in Eq. (12), which is 0.9, is very close to unity. Therefore, the depth can be approximately estimated by the following simplified relationship:

$$h = m(H-z) \quad (13)$$

$$m = \frac{h}{H-z} \approx \frac{n^{0.6} C^{0.6}}{J^{0.3}} \quad (14)$$

$m$  is called the water drop ratio which has sound physical meaning. The value of  $m$  can therefore be assigned based on experience. Chen et al. [1] found that the calculated peak flow is not sensitive to the value of  $m$ , if it is between 0.5 and 0.8. The velocity can then be determined by

$$V = \frac{C(H-z)^{3/2}}{h} \quad (15)$$

## 4.2 Algorithm

The breach hydrograph can be obtained by solving the equations in Sect. 4.1. However, they are highly nonlinear and coupled; the authors' following treatments have greatly facilitated the numerical algorithm.

**Integration Based on Velocity Increments.** Equations (1), (9), and (15) allow  $H$ ,  $z$ , and  $V$  to be solved at a particular time step  $\Delta t$ . However, these equations are highly nonlinear with concerns of numerical tractability. The new method performs the integration based on a velocity increment that completely linearizes of the governing equations and leads to a straight forwards calculation for the flow hydrograph.

At the velocity step from  $V_o$  to  $V_o + \Delta V$ , the average velocity is

$$\bar{V} = V_o + \Delta V/2 \quad (20)$$

A variable  $s$  is defined as  $(\Delta z - \Delta H)$  which can be calculated by

$$s = \Delta z - \Delta H = 2\left(\frac{m\bar{V}}{C}\right)^2 - 2(H_o - z_o) \quad (21)$$

from which the average velocity can be determined by

$$\bar{V} = Cm^{-1}\sqrt{(H_o - z_o + \frac{s}{2})} \quad (22)$$

The increment in channel elevation  $\Delta z$  is first calculated by

$$\Delta z = \frac{s}{1 - L} \quad (23)$$

where

$$L = \frac{m\bar{V}B_o(H_o - z_o + 0.5s) - q}{\Phi(\bar{\tau})\dot{W}} \quad (24)$$

The other variables can be readily calculated once  $\Delta z$  is determined.

**Transition Through the Threshold at Peak Velocity.** The key technology of this new method includes a criterion that detects the threshold at which the velocity attains its maximum  $V_m$ . It has been found that both  $(1 - L)$  and  $s$  in Eq. (23) approach zero at this particular point. Equation (23) is not applicable due to the limited calculation precision provided by the computer. Instead,  $\Delta z$  is calculated based on the Taylor series expansion for a value of  $V_o$  less than  $V_m$  as follows:

$$V_o = V_m - \frac{dV}{dz}\Delta z + \frac{1}{2}\frac{d^2V}{dz^2}\Delta z^2 = V_m + \frac{1}{2}\frac{d^2V}{dz^2}\Delta z^2 \quad (25)$$

from which we obtain

$$\Delta z = \sqrt{\frac{2(V_o - V_m)}{d^2V/dz^2}} = \sqrt{-\frac{2\Delta V}{d^2V/dz^2}} \quad (26)$$

In DB-IWHR, Eq. (26) will be used when the spread sheet calculation finds the value  $L$  is sufficiently close to unity, in a range between 0.985 and 1.015. Figure 8 gives the flow chart of the algorithm [37].

### 4.3 Computer Software

The numerical algorithm has been realized by an Excel spreadsheet supported by VBA. To assist in inputting the required parameters, the spreadsheet ‘Input’ will guide a user to fill up the cells as described in Fig. 9. They are self-explanatory, requiring minimal tutorials. By pushing the bottom “Back to ‘Calculation’ sheet”, the software turns to the main sheet ‘Calculation’.

In sheet ‘Calculation’, the user will check the input and press ‘Re Calculation’ to start the computation (Fig. 10).

DB-IWHR and its illustrating examples are available for downloading at: <https://github.com/ChenZuyuIWHR/DB-IWHR>.

### 4.4 Suggested Values of Input for Preliminary Studies

Dam breaches often happen without early warning. This has made it difficult to perform field and laboratory tests to define the material properties. The following empirical ranges of various input parameters based on the authors’ experience have been suggested for field engineers in their quick response to an impending dam failure:

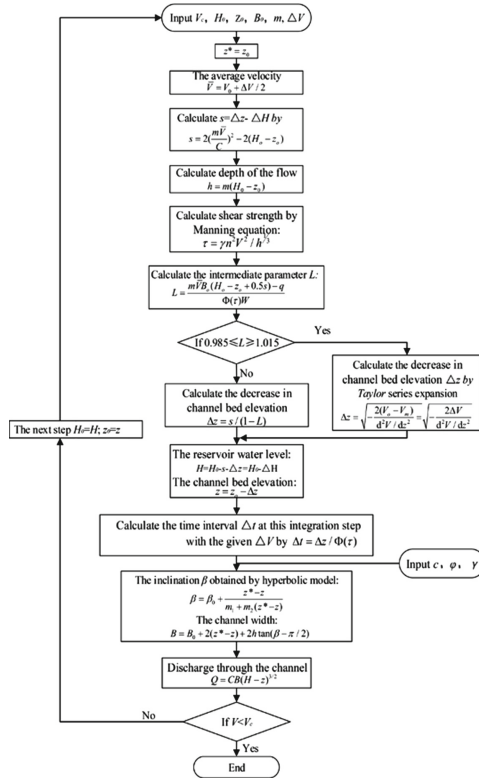


Fig. 8. Flow chart of the algorithm.

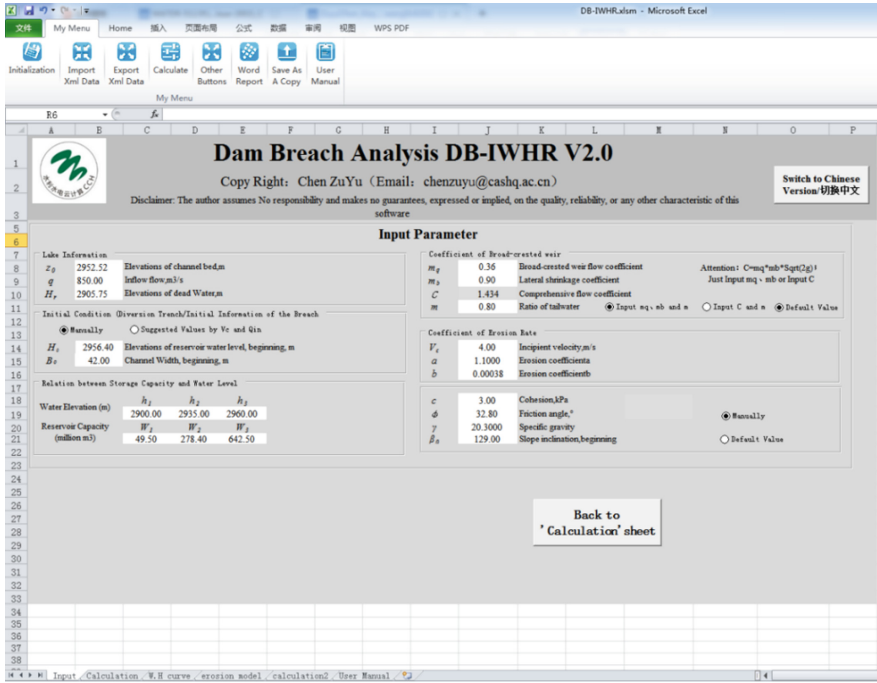


Fig. 9. Sheet ‘Input’ of DB-IWHR.

- (1) The discharge coefficient  $C$  of a broad-crested weir is between 1.3 and 1.7  $m^{0.5}/s$  [38]. For dams made of rock debris and earthen material, it may be taken to be around 1.45 and 1.50, respectively.
- (2) It has been suggested that the water head drop ratio,  $m$ , should be 0.5 [39, 40]. In view of the decreasing pool water level and the rising downstream riverbed elevation Chen et al. suggested a more reasonable range for  $m$  ranged between 0.8 and 0.6.
- (3) It is the responsibility of experienced geologists to suggest the dam material property parameters ( $\gamma$ ,  $c$ , and  $\phi$ ), but conducting quick and simple field or laboratory tests would be useful, if time permits.
- (4) Determining soil erosion parameters is the most difficult task. It is suggested to refer case records of similar nature and past experience. Table 1 gives some empirical suggestions for preliminary studies.


Table 1. Suggested values of  $a$  and  $b$  for preliminary studies [20].

Erodibility	Soil materials	$a$	$b$
1 Very high	Fine sand, Non-plastic silt	1.0	0.0001–0.0003
2 High	Medium sand, Low plasticity silt	1.1	0.0003–0.0005
3 Medium	Jointed rock (spacing < 30 mm), Fine gravel, Coarse sand, High plasticity silt, Low plasticity clay, All fissured clays	1.2	0.0005–0.0007

(continued)

Table 1. (continued)

	Erodibility	Soil materials	<i>a</i>	<i>b</i>
4	Low	Jointed rock (30–150 mm spacing), cobbles, Coarse gravel, High plasticity clay	1.3	0.0007–0.001
5	Very low	Jointed rock (150–1500 mm spacing), Riprap	1.3	0.001–0.01
6	Non-erosive	Intake rock, Jointed rock (spacing > 1500 mm)	1.3	0.01–0.1



## Dam Breach Analysis DB-IWHR V2.0

Copy Right: Chen ZuYu (Email: chenzuyu@cashq.ac.cn)

Disclaimer: The author assumes No responsibility and makes no guarantees, expressed or implied, on the quality, reliability, or any other characteristic of this software

Switch to Chinese Version/切换中文

Project Name	Serial Number	Calculated by	Checked by	Date	Company

**Lake Information**

*z<sub>0</sub>* 2952.52 Elevations of channel bed,m  
*q* 850.00 Inflow flow,m<sup>3</sup>/s  
*H<sub>v</sub>* 2905.75 Elevations of dead Water,m

---

**Relation between Storage Capacity and Water Level**

*p<sub>1</sub>* 0.13 W-H curve coefficient 1  Automatically  
*p<sub>2</sub>* 3.40 W-H curve coefficient 2  Manually  
*p<sub>3</sub>* 64.61 W-H curve coefficient 3

Note: obtained by water storage capacity curve worksheet

---

**Coefficient of Broad-crested weir**

*m<sub>q</sub>* 0.36 Broad-crested weir flow coefficient  Default value  
*m<sub>s</sub>* 0.90 Lateral shrinkage coefficient  
*m* 0.80 Ratio of tailwater  Manually

---

**Coefficient of erosion rate**

*V<sub>c</sub>* 4.00 Incipient velocity,m/s  
*a* 1.1000 Erosion coefficienta  Default value  
*b* 0.00038 Erosion coefficientb  
*τ<sub>c</sub>* 0.00 Incipient shear stress

input *H<sub>0</sub>*, *B<sub>0</sub>* and *z<sub>0</sub>* by

Manually  suggested values by *V<sub>c</sub>* and *Q<sub>in</sub>*

*H<sub>0</sub>* 2956.40 Elevations of reservoir water level, beginning, m  
*B<sub>0</sub>* 42.00 Channel Width, beginning, m

---

*c* 3.00 cohesion *m<sub>1</sub>* 0.0560 Lateral enlargement coefficient 1  
*φ* 32.80 friction angle *m<sub>2</sub>* 0.0308 Lateral enlargement coefficient 2  
*γ* 20.3000 Bulk Density  
*β<sub>0</sub>* 129.00 slope inclination,beginning  Default value  Manually

---

**sediment transport parameter**

*D<sub>50</sub>* 0.0050 Average particle size, m  
*ρ<sub>s</sub>* 2650.0000 Material density, kg/m<sup>3</sup>  
*v* 0.4300 Void ratio  
*G<sub>s</sub>* 2.6500 Specific gravity  
*L* 36.0000 Erosion length, m  
*n* 0.0250 Roughness of river

There are several candidate methods to consider the erosion rate of sediments. The User can switch the methods by click the Drop Down box

Lateral enlargement for the *h-t* ▼

Calculation button

Re calculate

**Peak Flow**

<i>W</i>	544.43	10 <sup>6</sup> m <sup>3</sup>	Total discharge capacity
<i>Q<sub>p</sub></i>	31041.09	m <sup>3</sup> /s	Magnitude
<i>t<sub>p</sub></i>	4.81	h	Time
Balance	1.48%		Balance

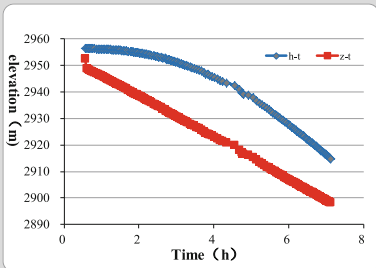


Figure 1

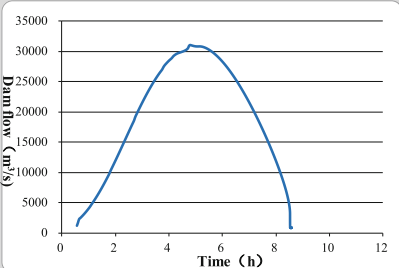


Figure 2

Fig. 10. Sheet 'Calculation' of DB-IWHR.

## 5 Case Study

### 5.1 Breach of Tangjiashan Barrier Lake

To illustrate the technical details described in this paper, this section uses the Tangjiashan landslide dam as a case study. The authors have in fact used this case previously [1] by investigating the breach hydrograph with the 13 m deep emergency diversion channel. This study, however, investigates the breach hydrograph without the emergency diversion channel. These comparative studies are useful when a decision has to be made.

The right part of the Tangjiashan dam is 105 m high with a crest elevation of 753 m above the sea level. The storage capacity of the reservoir is  $3.2 \times 10^9 \text{ m}^3$ . Construction of a diversion channel enables the water in the reservoir to be drained at the lower elevation of 740 m, thereby reducing the volume of released reservoir water to  $2.8 \times 10^9 \text{ m}^3$ . On one occasion after the reservoir water overflowed into the channel, the measured peak flow breaching the dam was  $6,500 \text{ m}^3/\text{s}$ , as compared to the peak flow of  $7,160 \text{ m}^3/\text{s}$  from the back analysis [1]. Various advanced instruments were used to measure the hydrograph of the breach, followed by a field survey and laboratory tests of geotechnical properties of the dam material [8]. This study continues the evaluation of the peak flow for the dam with no diversion channel, i.e., the reservoir water starts to drain at the elevation of 753 m.

**Target Case.** The inputs for the current case study are almost the same to the previous study and are summarized in Table 2.

**Table 2.** Input parameters for the current case study.

Item	$H_0$	$q_{in}$	$C$	$m$	$V_c$	$a$	$b$	$c$	$\phi$
Parameters	753 m	$80 \text{ m}^3/\text{s}$	1.43	0.8	2.7 m/s	1.2	0.0007	25 kPa	$22^\circ$

NOTE: The relationship between the pool water level and storage can be found in Liu et al. (2010) and is approximated by  $W = [p_1(H - H_r)^2 + p_2(H - H_r) + p_3] \times 10^6$  in  $\text{m}^3$ , where,  $p_1, p_2, p_3$  are 0.61, 1.983, 44 respectively, and  $H_r = 700$

Figure 6 shows the calculated results for the current case study with the inputs  $\gamma_{sat} = 24 \text{ kg/m}^3$ ,  $c' = 22^\circ$ , and  $\phi' = 25 \text{ kPa}$ . The model carried out the calculations for the 10 steps of circular failure to the elevation 727 m. After that, the width of the channel was not widened further because the rock of the right abutment was exposed as indicated by Chen et al. (2015). Figure 6(a) shows the processes of a typical failure.

For the current case study,  $z_{end} = 727 \text{ m}$  has been used to obtain  $B_{end} = 69 \text{ m}$ ,  $\beta_0 = 143^\circ$ , and  $\beta_{end} = 169.5^\circ$ . These results have been applied to Eq. (8) to determine the width of the water surface at a particular channel bed elevation.

**Illustration of the Computation.** Table 3 shows the condensed contents of DB-IWHR calculations.

**Table 3.** The condensed contents of DB-IWHR calculations.

1	2	3	4	5	6	7	8	9	10	11	12	13	14	15	16	17	18	19	20	21
	$H$	$z$	$V$	$B$	$Q$	$\Delta V$	$h$	$q$	Index	$V$	$s$	$\tau$	$L = \frac{L}{ADE}$	$\Delta z$	$\Delta z_{taylor}$	$H$	$z$	$\Delta t$	$t$	$S_{out}$
Unit	m	m	m/s	m	m <sup>3</sup> /s	m/s	m	m <sup>3</sup> /s		m/s	m	Pa	L	m	m	m	m	s	h	10 <sup>6</sup> m <sup>3</sup> /s
Eq.		(17)	(8)	(9)	(13)					(21)	(10)	(23)	(22)	(24)						(25)
61	753.000	750.428	2.700	16.2	98.4	0.080	2.06	80	1	2.780	0.154	36.2	0.004	0.155	0.155	752.999	750.273	384	0.11	0.0
62	752.999	750.273	2.780	28.1	145.3	0.08	2.18	80	1	2.860	0.146	37.6	0.025	0.149	0.149	752.996	750.124	322	0.20	0.0
63	752.996	750.124	2.853	28.8	202.5	0.08	2.30	80	1	2.933	0.163	38.9	0.027	0.167	0.167	752.991	749.957	325	0.29	0.1
:	:	:	:	:	:	:	:	:	:	:	:	:	:	:	:	:	:	:	:	:
132	746.161	732.686	6.180	130.6	8590.6	0.005	10.78	80	1	6.185	0.024	106.1	0.959	0.595	0.595	745.590	732.091	502	5.03	56.2
133	745.590	732.091	6.185	134.9	8893.6	0.005	10.80	80	1	6.190	0.024	106.2	1.003	-7.659	0.788	744.827	731.303	665	5.22	60.5
134	744.827	731.303	6.191	141.0	9222.2	0.005	10.82	80	-1	6.186	-0.020	106.1	1.062	0.314	0.314	744.493	730.989	265	5.29	66.5
135	744.493	730.989	6.186	143.4	9484.2	0.005	10.80	80	-1	6.181	-0.020	106.0	1.084	0.232	0.232	744.242	730.757	196	5.35	68.9
:	:	:	:	:	:	:	:	:	:	:	:	:	:	:	:	:	:	:	:	:
307	694.778	691.934	2.839	177.6	1123.5	0.02	2.28	80	-1	2.819	-0.040	37.3	1.730	0.054	0.054	694.685	691.880	120	16.14	288.7
308	694.262	691.651	2.720	177.6	987.4	0.02	2.09	80	-1	2.700	-0.038	35.2	2.010	0.038	0.038	694.187	691.614	106	16.33	289.5
309	694.187	691.614	2.701	177.6	965.8	0.02	2.06	80	-1	2.681	-0.038	34.9	2.081	0.035	0.035	694.114	691.579	103	16.36	289.6

NOTE: Index '1' and '-1' represent a positive and negative  $\Delta V$  respectively.  $\Delta z_{taylor}$  represents the value of  $\Delta V$  determined by (Eq. 26).

Line 61 starts the calculation with the conditions:  $H_0 = 753$  m,  $V_c = 2.7$  m/s,  $\Delta V = 0.08$  m/s,  $z_0 = 750.42$  m and  $B_0 = 16.23$  m. The calculated  $\Delta z$  as shown in Column 15 is 0.155 m, with  $z = 750.273$  m,  $H = 752.999$  m,  $\Delta t = 384$  s for the next step, as shown in Columns 17, 18, and 19, respectively.

Line 62 performs the second round of integration based on the new values of  $H$ ,  $z$ , and  $V$ . The calculation proceeds until Line 133 at which the velocity reaches its peak value.

Line 133 represents the transition point after which a negative  $\Delta V$  has been assigned. The value of  $L$  is 1.003, which is close to unity (Column 14), and  $s$  is 0.024. Equation (23) results in an abnormal value of  $\Delta z = -7.659$  m (Column 15), which is due to the insufficient precision in performing the division between two very small values by Eq. (23). Hence, the Taylors formulation (Eq. 26) was used, giving  $\Delta z = 0.788$  m (Column 16).

Line 134 continues the integration with the negative input of  $\Delta V$ .

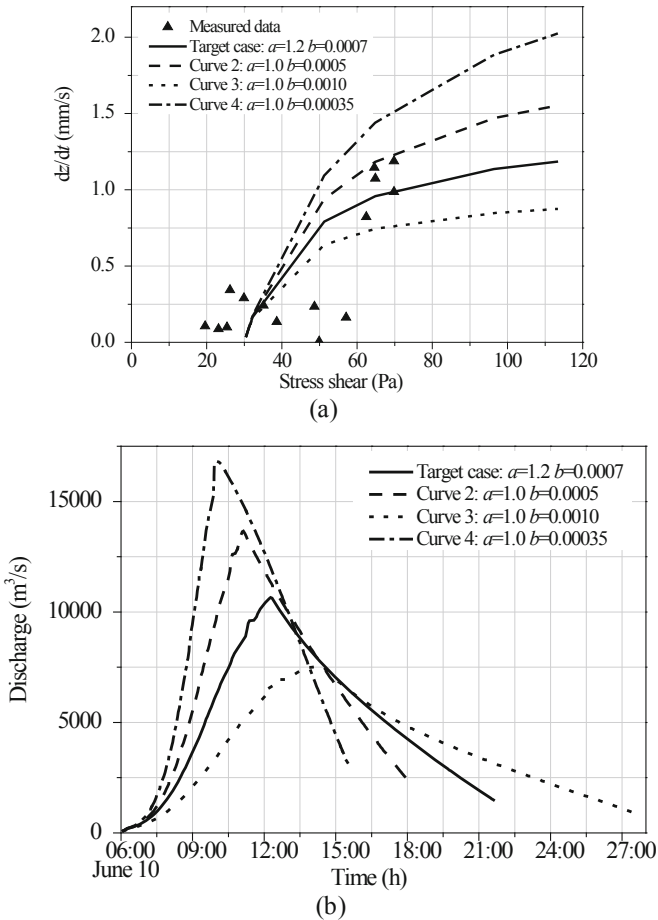


**Fig. 11.** Case study Calculations: (a) regressions for the erosion parameters (b) flow discharge.



Line 309 indicates the termination of the calculation at  $V = 2.701$  m/s which is equal to the incipient  $V_c$  of 2.7 m/s, as specified by Eq. (26).

The Solid line in Fig. 11(b) shows the DB-IWHR calculation results of the target case.

## 5.2 Sensitivity Analyses

Due to the large number of uncertainties in a dam breach flood analysis, investigation on the impact of different input values is considered as part of the analytical work. In the target case with the channeled dam, Chen et al. [1] performed the sensitivity analyses on six parameters  $C$ ,  $m$ ,  $a$ ,  $b$  and  $c$ ,  $\phi$ . This study has added one more parameter, the initial breach width  $B_0$ . Four sets of 'a and b' based on the measured data have been selected as shown in Fig. 11(a). Curve 1 (the target case), 2, 3 represent the mean, upper and lower bound of the regressions. Curve 4 is a postulated one whose value of  $1/b$ , the maximum possible erosion rate, is doubled to the target case. The results shown in Table 4 indicate that  $1/b$  is the most sensitive parameter, compared to the others.

A comparative study has been given to a linear model as described by Eq. (2). Following the similar process, three sets of  $a_L$  have been selected representing the mean, upper and lower bound of the regressions as shown in Fig. 12(a). Figure 12(b) shows the calculated hydrographs that display quite large deviations both in terms of the shape

**Table 4.** Sensitivity analyses based on various characteristic parameters.

Variable	Value		Occurring time	Discharge	Deviation
			$t_m$ (h)	$Q_m$ (m/s)	%
	Target case	Sensitivity studies			
Initial width of the breach, $B_0$ (m)	16	30	12:19	10286.76	-3.6%
		50	12:23	9796.24	-8.81%
Ratio of water head drop, $m$	0.8	0.5	9:29	11198.60	4.8%
		0.6	11:28	11366.13	6.2%
Coefficient of broad-crested weir flow, $C$	1.43	$C_I = 1.35$	12:20	10605.05	-0.5%
		$C_I = 1.65$	14:28	10258.95	-3.9%
Coefficient of soil erosion, $a$ and $b$	$a = 1.2$ , $b = 0.0007$	$a = 1.0$ , $b = 0.0005$	11:08	13,664.90	22.0%
		$a = 1.0$ , $b = 0.0010$	14:26	7,536.02	-41.4%
		$a = 1.0$ , $b = 0.00035$	10:02	16818.08	38.8%
Cohesion and friction angle, $c$ (kPa) and $\phi$ (°)	$\phi = 22^\circ$ $c = 25$ kPa	$c = 25$ kPa $\phi = 26^\circ$	12:23	9705.51	-9.83%
		$c = 35$ kPa $\phi = 22^\circ$	12:22	9546.29	-11.66%

NOTE:  $Q_m$  = peak flow,  $t_m$  = time at peak flow, Deviation =  $(Q_m - Q_{m,t})/Q_m$ , where  $Q_{m,t}$  is 10,659 m<sup>3</sup>/s, the peak flow of the target case.

and the magnitude of peak flow. The previous report [1] discussed the concerns on sensitivities related to the power relation model. This gives a reason of adopting the hyperbolic model (Fig. 12).

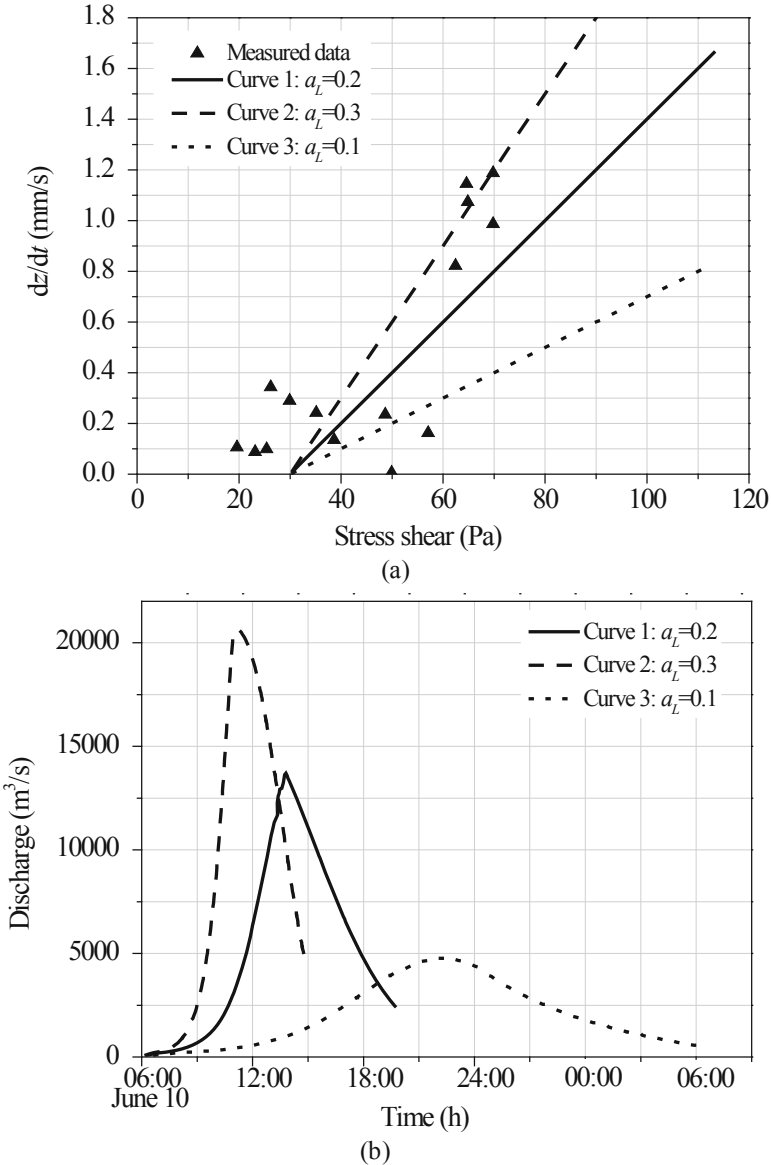


**Fig. 12.** Sensitivity study calculations with the linear model: (a) regressions for the erosion parameters. (b) flow discharge.

## 6 Conclusions

The improvements to the existing dam breach analysis methods described in this paper include a new soil erosion model, an empirical hyperbolic model for lateral enlargement modeling, and a novel numerical algorithm that allows straight forward calculation for the breach flood hydrograph. The new method has been incorporated into the Excel spreadsheets DB-IWHR, which perform the dam breach flood calculation and the lateral enlargement calculation respectively. These spreadsheets are transparent, self-explanatory and ready for group sourcing development on the web. The main highlights are:

- (1) The hyperbolic soil erosion model developed in this study includes the parameter  $1/a$  which is close to the relevant coefficient in the traditional linear model, and the parameter  $1/b$  which is a 'truncation' at large shear stress. The new model makes the calculated peak flow less sensitive to the input parameters. In addition, these two parameters have sound physical meaning. Therefore, with increased knowledge, their applicable values for various soils can be improved in practice. As a new model with limited experience of practical application, the authors would suggest users be cautious when using this model. It is advantageous to adopt different soil erosion models and make comparative studies. DB-IWHR allows another 5 representative models for users to select.
- (2) The procedures of modeling lateral enlargement has been updated by modern geotechnical expertise on slope stability analysis. However, the solutions have been simplified to a series of trapezoidal cross sections in order to facilitate the calculation without substantial loss in accuracy.
- (3) The new method developed in this study uses velocity increment during the integration of the governing equations, thus allowing a straightforward solution. The calculation procedure has been incorporated into an Excel spreadsheet, providing easy, transparent access to practitioners.
- (4) The results of this study show that the erosion rate parameter  $1/b$  is the most sensitive input that affects the calculated peak flow. Other parameters are less sensitive, which only cause 5 to 10% variations in the peak flow.

## References

1. Chen, Z.Y., Ma, L.Q., Yu, S., Chen, S.J., Zhou, X.B., Sun, P., Li, X.: Back analysis of the draining process of the Tangjiashan barrier lake. *J. Hydraul. Eng.* **141**(4), 05014011 (2015)
2. Cristofano, E.A.: Method of Computing Erosion Rate of Failure of Earth Dams. U.S. Bureau of Reclamation, Denver (1965)
3. Harris, G.W.: Outflow from breached earth dams. Doctoral Dissertation, Department of Civil Engineering, University of Utah, Salt Lake City (1967)
4. Brown, R.J., Rogers, D.C.: A simulation of the hydraulic events during and following the Teton Dam Failure. In: Proceedings of Dam-Break Flood Routing Workshop, Washington, DC, pp. 131–163 (1977)

5. Fread, D.L.: BREACH: An Erosion Model for Earthen Dam Failures (Model Description and User Manual). National Oceanic and Atmospheric Administration, National Weather Service, Silver Spring (1988)
6. Wu, W.M.: Simplified physically based model of earthen embankment breaching. *J. Hydraul. Eng.* **139**(8), 837–851 (2013)
7. Chen, Z., Zhang, Q., Chen, S., Wang, L., Zhou, X.: Evaluation of barrier lake breach floods: insights from recent case studies in China. *Wiley Interdiscip. Rev.: Water* **7**(2) (2020). <https://doi.org/10.1002/wat2.1408>
8. Liu, N., Chen, Z.Y., Zhang, J.X., Wei, L., Chen, W., Xu, W.J.: Draining the Tangjiashan barrier lake. *J. Hydraul. Eng.* **136**(11), 914–923 (2010)
9. Zhou, X.B., Chen, Z.Y., Yu, S., Wang, L., Deng, G., Sha, P.J., Li, S.Y.: Risk analysis and emergency actions for Hongshiyuan barrier lake. *Nat. Hazards* **79**(3), 1933–1959 (2015)
10. Chen, Z.Y., Chen, S.S., Wang L., Zhong Q., Zhang Q., Jin, S.L.: Evaluation of the breach flood of the “11.03” Baige barrier lake at the Jinsha River. *Sci. China Tech. Sci.* (2020). <https://doi.org/10.1360/sst-2019-0297>. (in Chinese)
11. Cai, Y.J., Cheng, H.Y., Wu, S.F., Yang, Q.G., Wang, L., Luan, Y.S., Chen, Z.Y.: Breaches of the Baige Barrier Lake: emergency response and dam breach flood. *Sci. China Technol. Sci.* (2019). <https://doi.org/10.1007/s11431-019-1475-y>
12. Hanson, G.J.: Channel erosion study of two compacted soils. *Trans. ASAE* **32**(2), 485–490 (1989)
13. Zhang, L.M., Peng, M., Chang, D.S., Xu, Y.: *Dam Failure Mechanisms and Risk Assessment*. Wiley, Singapore (2016)
14. Smart, G.M.: Sediment transport formula for steep channels. *J. Hydraul. Eng.* **110**(3), 267–276 (1984)
15. Brown, C.B.: Sediment transportation. In: Rouse, H. (ed.) *Engineering Hydraulics*, pp. 711–768. Wiley, New York (1950)
16. Singh, V.P.: *Dam breaching modeling technology*. Kluwer Academic Publishers, Dordrecht, Netherlands (1996)
17. Engelund, F., Hansen, E.: A monograph on sediment transport in alluvial streams. *Hydrotech. Constr.* **33**(7), 699–703 (1967)
18. Roberts, J., Jepsen, R., Gotthard, D., Lick, W.: Effects of particle size and bulk density on erosion of quartz particles. *J. Hydraul. Eng.* **124**(12), 1261–1267 (1998)
19. Zhou, X.B., Chen, Z.Y., Li, S.Y., Wang, L.: Comparison of sediment transport model in dam break simulation. *J Basic Sci. Eng.* **23**(6), 1097–1108 (2015). (in Chinese)
20. Chen, Z.Y., Ma, L.Q., Yu, S., Chen, S.J., Zhou, X.B., Sun, P., Li, X.: Closure to “back analysis of the draining process of Tangjiashan barrier lake” by Zuyu Chen, Liqiu Ma, Shu Yu, Shujing Chen, Xingbo Zhou, Ping Sun, and Xu Li. *J. Hydraul. Eng.* **142**(6), 07016002 (2016)
21. Foster, G.R., Meyer, L.D., Onstad, C.A.: An erosion equation derived from basic erosion principles. *Trans. ASAE* **20**(4), 678–682 (1977)
22. Temple, D.M.: Stability of grass lined channels following mowing. *Trans. ASAE* **28**(3), 750–754 (1985)
23. Shaikh, A., Ruff, J.F., Abt, S.R.: Erosion rate of compacted Na-montmorillonite soils. *J. Geotech. Eng.* **114**(3), 296–305 (1988)
24. Hanson, G.J., Simon, A.: Erodibility of cohesive streambeds in the loess area of the midwestern USA. *Hydrol. Process.* **15**(1), 23–38 (2001)
25. Wan, C.F., Fell, R.: Investigation of rate of erosion of soils in embankment dams. *J. Geotech. Geoenviron.* **130**(4), 373–380 (2004)
26. Zhu, Y.H., Lu, J.Y., Liao, H.Z., Wang, J.S., Fan, B.L., Yao, S.M.: Research on cohesive sediment erosion by flow: an overview. *Sci. China Ser. E.* **51**(11), 2001–2012 (2008)

27. Chang, D.S., Zhang, L.M.: Simulation of the erosion process of landslide dams due to overtopping considering variations in soil erodibility along depth. *Nat. Hazard Earth Syst. Sci.* **10**(4), 933–946 (2010)
28. Ma, L.Q.: Flood analysis of landslide dam breach. Post-Doctoral Dissertation, China Institute of Water Resources and Hydropower Research, Beijing (2014). (in Chinese)
29. Singh, V.P., Scarlatos, P.D.: Analysis of gradual earth-dam failure. *J. Hydraul. Eng.* **114**(1), 21–42 (1988)
30. Wang, L., Chen, Z.Y., Wang, N.X., Sun, P., Yu, S., Li, S.Y., Du, X.H.: Modeling lateral enlargement in dam breaches using slope stability analysis based on circular slip mode. *Eng. Geol.* **209**, 70–81 (2016)
31. Osman, A.M., Thorne, C.R.: Riverbank stability analysis. I: Theory. *J. Hydraul. Eng. ASCE* **114**(2), 134–150 (1988)
32. Duncan, J.: State of the art: limit equilibrium and finite-element analysis of slopes. *J. Geotech. Eng.* **122**(7), 577–596 (1996)
33. Chen, Z.Y., Shao, C.M.: Evaluation of minimum factor of safety in slope stability analysis. *Can. Geotech. J.* **25**(4), 735–748 (1988)
34. Sherard, J., Woodward, R., Gzienski, S., Clevenger, W.: Failures and damages. In: *Earth and Earth-Rock Dams*, 1st edn, pp. 130–131. Wiley, New York (1963)
35. Lowe, J., Karafiath, L.: Stability of earth dam upon drawdown. In: *First Pan-American Conference on Soil Mechanics and Foundation Engineering*, Mexico City, vol. 2, pp. 537–552 (1960)
36. Johnson, J.J.: Analysis and design relating to embankments. In: *Proceedings, Conference on Analysis and Design in Geotechnical Engineering*, vol. 2, pp. 1–48. ASCE, New York (1974)
37. Chen, Z.Y., Ping, Z.Y., Wang, N.X., Yu, S., Chen, S.J.: An approach to quick and easy evaluation of the dam breach flood. *Sci. China Tech. Sci.* **62**(10), 1773–1782 (2019)
38. Jack, R.: The mechanics of embankment failure due to overtopping flow. Doctoral dissertation, University of Auckland, Auckland, New Zealand (1996)
39. Chow, V.T.: *Open-Channel Hydraulics*. McGraw Hill, New York (1959)
40. Doeringsfeld, H.A., Barker, C.L.: Pressure momentum theory applied to the broad crested weir. *Trans. ASCE* **106**, 934–969 (1941)